

See discussions, stats, and author profiles for this publication at: <https://www.researchgate.net/publication/231652048>

CdTe Quantum Dots-Sensitized TiO₂ Nanotube Array Photoelectrodes

ARTICLE *in* THE JOURNAL OF PHYSICAL CHEMISTRY C · APRIL 2009

Impact Factor: 4.77 · DOI: 10.1021/jp810727n

CITATIONS

173

READS

211

6 AUTHORS, INCLUDING:



Xianfeng Gao

University of Wisconsin - Milwaukee

25 PUBLICATIONS 1,136 CITATIONS

[SEE PROFILE](#)



Qing Chen

Peking University

173 PUBLICATIONS 6,004 CITATIONS

[SEE PROFILE](#)



Lian-Mao Peng

Peking University

396 PUBLICATIONS 9,731 CITATIONS

[SEE PROFILE](#)

Article

CdTe Quantum Dots-Sensitized TiO₂ Nanotube Array Photoelectrodes

Xian-Feng Gao, Hong-Bo Li, Wen-Tao Sun, Qing Chen, Fang-Qiong Tang, and Lian-Mao Peng

J. Phys. Chem. C, **2009**, 113 (18), 7531-7535 • Publication Date (Web): 08 April 2009

Downloaded from <http://pubs.acs.org> on April 30, 2009

More About This Article

Additional resources and features associated with this article are available within the HTML version:

- Supporting Information
- Access to high resolution figures
- Links to articles and content related to this article
- Copyright permission to reproduce figures and/or text from this article

[View the Full Text HTML](#)



ACS Publications

High quality. High impact.

The Journal of Physical Chemistry C is published by the American Chemical Society. 1155 Sixteenth Street N.W., Washington, DC 20036

CdTe Quantum Dots-Sensitized TiO₂ Nanotube Array Photoelectrodes

Xian-Feng Gao,[†] Hong-Bo Li,[‡] Wen-Tao Sun,[†] Qing Chen,[†] Fang-Qiong Tang,[‡] and Lian-Mao Peng^{*,†}

Key Laboratory for the Physics and Chemistry of Nanodevices and Department of Electronics, Peking University, Beijing 100871, China, and Laboratory of Controllable Preparation and Application of Nanomaterials, Technical Institute of Physics and Chemistry, Chinese Academy of Sciences, Beijing 100080, China

Received: December 6, 2008; Revised Manuscript Received: March 18, 2009

TiO₂ nanotube array films, formed by anodic oxidation, have been shown to yield high efficiency of charge generation and collection in photoelectrochemical (PEC) devices. However, the wide band gap (3.2 eV) of TiO₂ limits the efficiency of these devices in the visible region. In this work, four types of presynthesized CdTe quantum dots (QDs) of different sizes were deposited into the TiO₂ nanotubes to serve as the sensitizers, and the performance of the CdTe QD-sensitized TiO₂ nanotube arrays was measured in a PEC solar cell. It is found that, with decreasing particle size, the driving force for electron injection increases while the visible light response decreases. Maximum photocurrent was obtained for the QDs that have an absorption peak at 536 nm. Under AM 1.5 G illuminations, a 6 mA/cm² short circuit current density is achieved, which presents a 35 times improvement compared to that based on using a plain TiO₂ nanotube film.

Introduction

Since the phenomenon of photocatalytic splitting of water on TiO₂ electrodes was discovered in 1972,¹ extensive investigations have been devoted to improve the photocatalytic efficiency of TiO₂-based photoelectrodes. In particular regular TiO₂ nanotube arrays have been fabricated and used for water cleavage,^{2,3} and for developments of gas sensors⁴ and dye-sensitized solar cells.^{5–7} The highly ordered TiO₂ nanotube arrays exhibited good performance when used as a photoelectrode, due to the unique nanostructure that facilitates separation of the photoexcited charges and results in higher charge collection efficiencies.⁷ However, it is well-known that TiO₂ has a wide band gap of 3.2 eV, preventing efficient absorption of the sunlight in the visible region. A promising solution to this problem is to combine TiO₂ with dye molecules or narrow band gap semiconductors of suitable band gaps to extend the absorption range of TiO₂. Comparing with other sensitizers, semiconductor quantum dots (QDs) have two unique advantages. First, the band gap of the QDs can be modified by varying the size of the QDs allowing one to tune the visible response of the QDs. Second, QDs can be used to utilize hot electrons or to generate multiple charge carriers with a single high-energy photon.⁸ Various semiconductor QDs, including CdS,^{9–11} PbS,^{9,12} Bi₂S₃,^{9,13} CdSe,^{14,15} and InP,¹⁶ have been investigated to sensitize TiO₂ as a visible light absorber. However, little detailed investigation has been devoted to CdTe, which is one of the most important absorption materials for thin film solar cells. CdTe is a direct band gap semiconductor with $E_g = 1.5$ eV, close to the optimum for photoconversion, and a very high optical absorption material. It is among the few II–VI compounds that can be doped p-type and n-type, and it is in principle best suited for photovoltaic applications.

In an earlier paper we reported that the photoelectric conversion efficiency of the TiO₂ nanotube array film can be significantly improved by the introduction of CdS QDs inside the TiO₂ nanotubes by sequential chemical bath deposition method.¹¹ However, the size of the QDs is difficult to control via this method in order to fully utilize the benefits of QDs. In this paper, we show that presynthesized CdTe QDs by the solution deposition method can be introduced into the TiO₂ nanotubes and be utilized to sensitize and improve significantly the performance of the TiO₂ nanotube array-based photoelectrochemical (PEC) solar system. In particular the photocurrent response of the electrode is shown to have been improved from 0.17 mA/cm² to 6 mA/cm².

Experimental Section

Preparation of CdTe QDs. CdTe QDs were synthesized via a method similar to that described by Gao et al.^{17,18} but with minor modifications. Briefly, the CdTe precursor solution was prepared by adding freshly prepared NaHTe solution to a nitrogen-saturated CdCl₂ solution at pH 10.0 in the presence of mercaptopropionic acid (MPA) as stabilizer. The precursor concentrations were [Cd] = 1.0 mmol/L, [MPA] = 1.4 mmol/L, and [Te] = 0.5 mmol/L, respectively. The CdTe precursor solution was heated at 80 °C for various times, yielding QDs with sizes between 2 and 6 nm. A longer heating time results in a larger particle size.

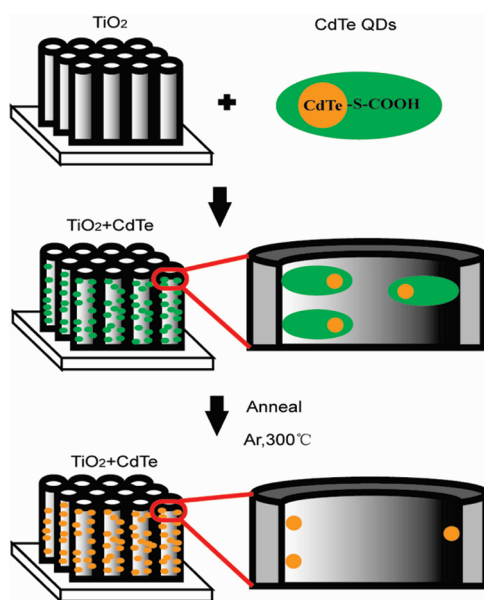
TiO₂ Nanotube Arrays. The highly ordered TiO₂ nanotube films were synthesized by anodic oxidation in NH₄F organic electrolyte, which is similar to that described by Macak et al.^{19,20} After oxidation, the sample was washed in ethanol to remove precipitation atop the nanotube film. The so obtained highly ordered TiO₂ nanotube film was converted to anatase phase by annealing in air for 2 h at 450 °C with a heating rate of 3 deg/min.

Linking CdTe QDs with TiO₂ Nanotube Arrays. As TiO₂ has a strong affinity for the carboxylate group of the linker molecules, bifunctional linker molecules (HOOC-R-SH) with

* To whom correspondence should be addressed. E-mail: Impeng@pku.edu.cn.

[†] Peking University.

[‡] Chinese Academy of Sciences.

SCHEME 1: The Process of Linking CdTe QDs to TiO₂

carboxylate and thiol functional groups were used to facilitate the binding of CdTe QDs to TiO₂. Such an approach has been used to link CdSe¹⁵ and Au nanoparticles²¹ to TiO₂ successfully. In the reported papers QDs used for photovoltaic devices were prepared via hot-injection techniques.^{15,22} The obtained QDs were hydrophobic and dispersed in organic solvent. Before linking the QDs with TiO₂, the QDs should be modified with MPA, which contains one mercapto group and one carboxylate group.¹⁵ Alternatively the surface of TiO₂ was modified with MPA to link the hydrophobic QDs with TiO₂.²³ Modifying the surface of TiO₂ with 16-mercaptopentadecanoic acid was also reported.²⁴ In this work, the CdTe QDs were synthesized by aqueous colloid approach as previously described.^{17,18} The obtained CdTe QDs were capped with MPA. The mercapto group is conjugated with the Cd²⁺ ion on the surface of CdTe QDs, while the carboxylate group will be ionized in the water to make the CdTe QDs water soluble. The obtained QDs were directly absorbed by the TiO₂ due to the carboxylate group. There is no need to modify the QDs or the surface of TiO₂. On the other hand, the TiO₂ nanotube is hydrophilic after conversion to anatase,²⁵ the synthesized aqueous CdTe QDs here were convenient for modifying the TiO₂ nanotubes, which also ensure enough QDs deposited on TiO₂ nanotubes. So CdTe QDs prepared via the aqueous colloid approach are attractive to sensitize the TiO₂ nanotube arrays.

In our experiments, the TiO₂ nanotube film was immersed in the solution of CdTe QDs and the film was kept in the solution for 2 h. The resulting TiO₂ film, linked with CdTe QDs, was then washed with deionized water and dried in air. This process was repeated several times to ensure that enough CdTe quantum dots were incorporated into TiO₂ nanotubes. After modification with CdTe QDs, the TiO₂ film was annealed at 300 °C in argon for 30 min to improve the CdTe/TiO₂ interface and to vaporize the linking molecules (Scheme 1).

Morphology, Optical, and Electrochemical Measurements. The structural characterizations of the samples were carried out with a field-emission gun FEI XL30 scanning electron microscope (SEM) and a Tecnai G20 transmission electron microscope (TEM).

Absorption spectra were obtained by using a Shimadzu UV-3100 spectrophotometer. Emission spectra were recorded on an Acton SP2358 spectrometer under 442 nm excitation.

The electrophotovoltaic performance of the CdTe QDs-sensitized TiO₂ nanotube film was measured in a PEC cell. The photocurrent density–voltage (*J*–*V*) characteristics measurements were performed under AM 1.5 simulated sunlight, which was produced by a 300-W Oriel Solar Simulator (Model, 91160) with an illumination intensity of 138.4 mW/cm². An electrochemical analyzer (CHI660C Instruments) was used to measure the PEC response of the sample, with a conventional three-electrode system comprised of an Ag/AgCl reference electrode, a Pt thread counter electrode, and the sample electrode. All potentials are reported relative to the Ag/AgCl reference electrode. A 0.1 M Na₂S aqueous solution was used as the electrolyte.

Results and Discussion

Characterization of the CdTe QDs. Four samples of CdTe QDs with different sizes and therefore different first excitonic peaks at 520, 536, 560, and 580 nm were used in the present study, and we refer to them as Q1–Q4 in our following discussions. For reference, the absorption and PL spectra obtained from the four different-sized CdTe QDs are shown in Figure 1. With decreasing particle size, the onset absorption of visible lights shifts toward the lower wavelength, as does the corresponding emission spectrum. This phenomenon represents size quantization effects in QDs. For comparison with the QDs after being deposited into the TiO₂ nanotubes, the sizes of the QDs are also characterized by dispersing the QDs on an amorphous carbon supporting film. Shown in Figure 2 is the TEM image of CdTe QDs with an absorption peak at 536 nm (Q2). The size of the QDs (Q2) is found to be around 4 nm. The inset of Figure 2 is a high-resolution TEM (HRTEM) image showing that the QDs are indeed single crystalline.

Morphology of the TiO₂ Nanotube Arrays before and after Sensitization. SEM and TEM images of TiO₂ nanotube arrays were taken before and after being modified with CdTe QDs (Q2). Figure 3a is a low-magnification SEM image showing a typical well-ordered TiO₂ nanotube array sample with an average nanotube diameter of about 130 nm. Figure 3b is a cross-sectional view of the same sample, showing that the nanotubes are about 11.3 μm in length and are well aligned vertically on a Ti film. Shown in panels c and d of Figure 3 are low- and high-magnification TEM images of the TiO₂ nanotubes after the incorporation of CdTe QDs. The nanotube structures are seen to be intact, i.e., they are not damaged during the CdTe deposition process. The HRTEM image of a single nanotube (Figure 3e) shows that individual QDs are dispersed onto the inner wall of the tube. The size of the CdTe QDs is basically in agreement with that shown in Figure 2, indicating that the sensitizing process did not cause aggregation of CdTe nanoparticles. The observed lattice fringes of 0.352 nm in the image (Figure 3e) correspond to the (101) plane of anatase (JPCDS 71-1166), suggesting that the side wall of the TiO₂ nanotube is well crystallized. The observed lattice spacing 0.282 and 0.262 nm of the QDs in the nanotube correspond to the (100) and (011) planes of CdTe (JPCDS 41-0941). These results confirm that CdTe QDs have been successfully assembled into the TiO₂ nanotube arrays.

Optical and Photoelectrochemistry Property of a QDs-Sensitized TiO₂ Nanotube Array. Shown in Figure 4 are UV-vis absorption spectra obtained from TiO₂ nanotube films before and after the deposition of CdTe QDs (with an absorption peak at 536 nm). The spectrum obtained from the plain TiO₂ nanotube film (Figure 4, curve a) shows that TiO₂ nanotubes absorb mainly the ultraviolet light with a wavelength below 400

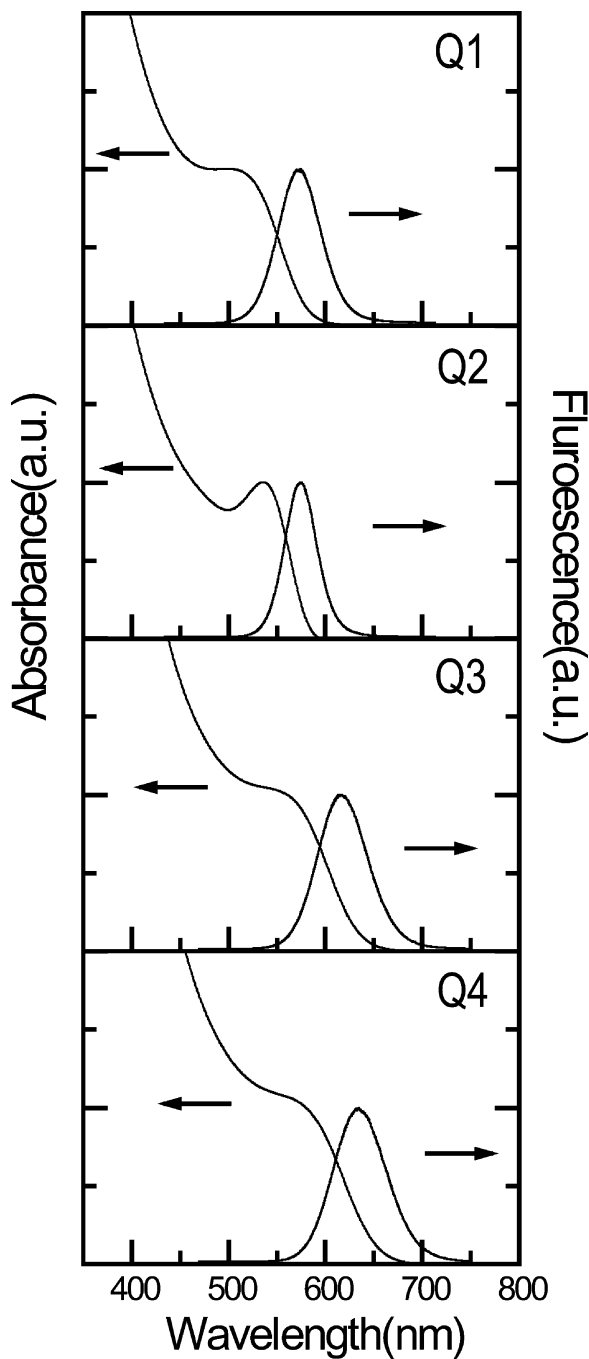


Figure 1. Absorption and emission spectra of CdTe QDs (Q1–Q4). Emission spectra were recorded with 442 nm excitation.

nm. After the deposition of CdTe QDs in the film, the absorption spectrum shows that the absorption edge is shifted significantly toward the visible region (Figure 4, curve b). This red shift is consistent with the feature shown in Figure 3 that CdTe QDs are added to the TiO₂ nanotube film inducing an absorption peak at about 536 nm. By depositing presynthesized CdSe QDs into the TiO₂ nanotube, a similar improvement of absorption property which is attributed to the CdSe QDs is also seen.²³ Furthermore, by in situ growth of CdS in the TiO₂ nanotube, the absorption spectrum of the TiO₂ film was extended into the visible region with a band edge of 510 nm.²⁶ Seabold et al. have also filled the TiO₂ tubes with CdTe by an electrochemical method, which present a bandgap transition at 1.48 eV.²⁷ All these results confirm that the incorporated QDs can improve the visible light absorption property of the TiO₂ photoelectrode effectively.

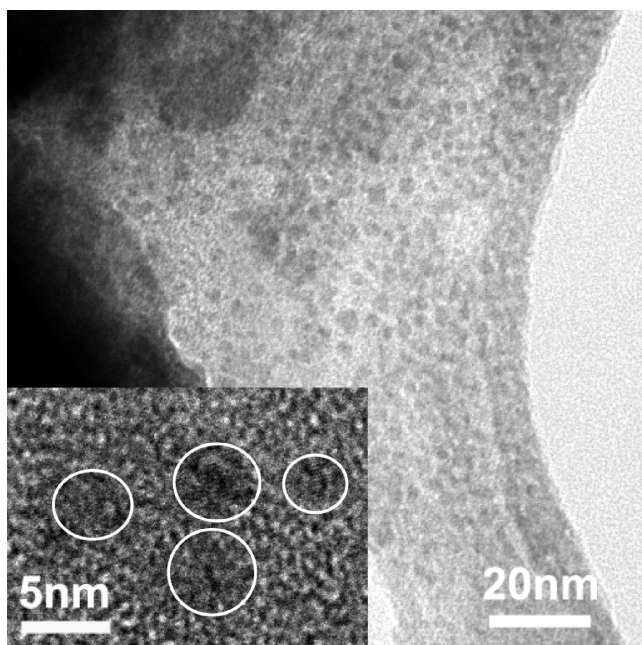


Figure 2. TEM and HRTEM (inset) images of CdTe QDs (Q2).

Figure 5 shows emission spectra obtained from CdTe QDs (Q2) before and after being deposited into the TiO₂ nanotubes. Shown in Figure 5a, the QDs exhibit characteristic emission peaks at 573 nm. After the QDs are deposited into the TiO₂ nanotube, the hybrid nanostructure exhibits the same emission peak as the origin QDs, but the emission is significantly quenched (Figure 5, curve b). The quenching behavior confirms that most of the excited electrons in CdTe QDs had been transferred to the TiO₂ nanotube, significantly improving the photovoltaic performance of the system.

The experimental *J*–*V* characteristics measured from the TiO₂ nanotube films are presented in Figure 6. For the plain TiO₂ nanotube film electrode, the photocurrent onset occurs at -0.94 V versus the Ag/AgCl electrode, while for the CdTe-sensitized TiO₂ nanotube film electrode, the photocurrent onset is shifted to -1.21 ± 0.01 V, suggesting a significant increase in the open voltage of the cell compared to the plain TiO₂ nanotube film electrode. The generated short-circuit photocurrent is increased from 0.17 mA/cm² (curve a in Figure 6, for the plain TiO₂ nanotubes) to 1.68 ± 0.06 mA/cm² (curves b–e in Figure 6, for the CdTe QDs-sensitized TiO₂ nanotubes). This presents a 10 times increase in the photocurrent response after the incorporation of the CdTe QDs in the TiO₂ nanotube film.

According to the UV–vis spectra of Figure 4, the incorporation of CdTe QDs into TiO₂ nanotubes extends the absorption spectrum of the plain TiO₂ film significantly into the visible region. When illuminated, CdTe QDs effectively absorb visible lights (with absorption peak centers at 536 nm) and excite electrons and holes pairs. Since the conduction band edge of CdTe QDs is above that of the TiO₂ nanotube, local band bending occurs at the TiO₂/CdTe interface, which results in a local electric field pushing the photon generated electrons toward the conduction band of TiO₂ (Scheme 2). Since the TiO₂ nanotubes are crystalline and well aligned on the Ti substrate, the injected electrons can be transferred effectively to the collector electrode (the Ti substrate foil). Therefore, the CdTe QDs-sensitized TiO₂ nanotube array photoelectrode has a higher photocurrent than that of the plain TiO₂ nanotube array.

Another important point that emerges from Figure 6 is the photocurrent response varies with different-sized QDs. The

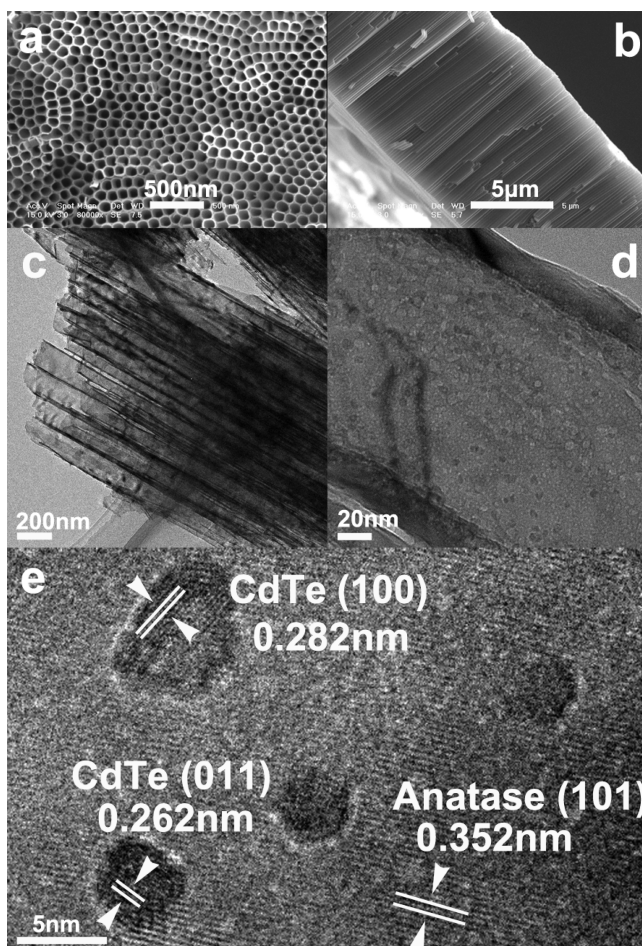


Figure 3. Morphology of TiO_2 nanotubes and CdTe QDs (Q2). SEM images showing (a) a top view and (b) a cross-section view of the well-aligned TiO_2 nanotube film sample. (c) Low- and (d) high-magnification TEM images showing TiO_2 nanotubes after the CdTe QDs deposition. (e) High-resolution TEM image showing individual CdTe QDs dispersed on the wall of a TiO_2 nanotube.

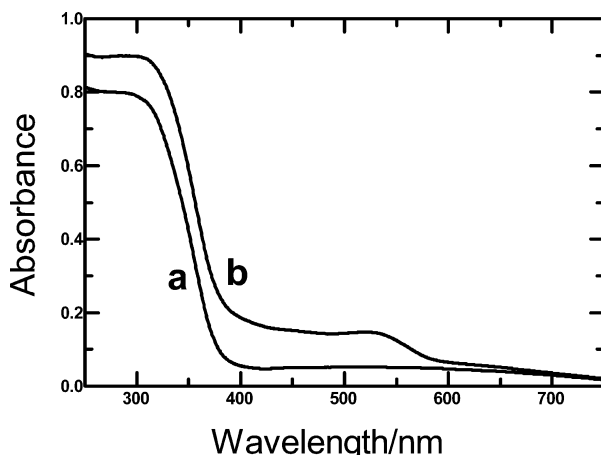


Figure 4. UV-vis absorption spectra measured from (a) a plain TiO_2 nanotube array electrode; (b) CdTe QDs (Q2)-modified TiO_2 nanotube array electrode.

maximum short-circuit photocurrent is seen with the Q2-sensitized photoelectrode. This result can be explained by the size quantization effects in these nanoparticles. Controlling particle size offered a method of changing the band energies, and therefore modulating the energy of the charge carriers. Because of the small electron effective mass ($m_e = 0.13 m_0$

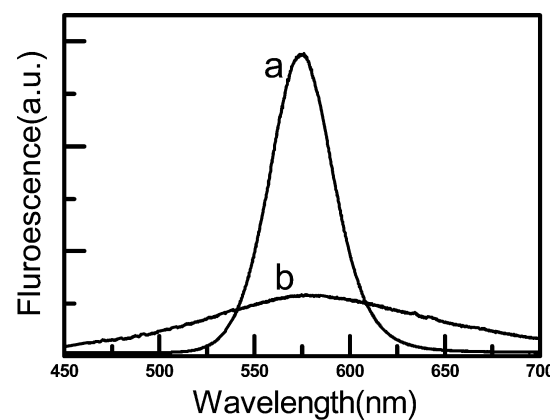


Figure 5. Emission spectra obtained from (a) CdTe QDs (Q2) and (b) CdTe QDs (Q2)-sensitized TiO_2 nanotube array electrode.

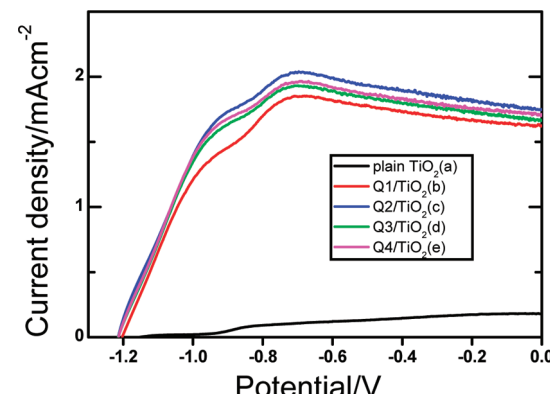
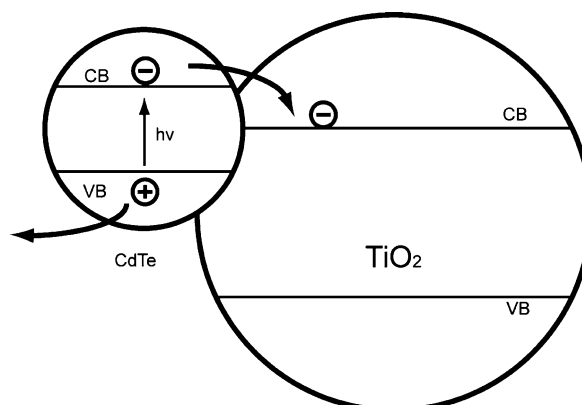


Figure 6. Current density–voltage characteristics measured from (a) plain TiO_2 nanotube film and CdTe QD with visible light absorption peaks of (b) 520, (c) 536, (d) 560, and (e) 580 nm modified TiO_2 nanotube film.

SCHEME 2: Charge Transfer Process between CdTe QDs and TiO_2



versus the significantly larger hole mass ($m_h = 1.14 m_0$), most of the band gap increase is seen as a shift in the conduction band to more negative potentials versus NHE.^{28,29} This negative potential shift of the conduction band increases the driving force for charge injection. As a result, smaller CdTe QDs have higher rates to inject electrons to TiO_2 . On the other hand, the bandgap of the QDs increased with the decreasing of the QDs size, which lowers the photocurrent due to an inherently smaller absorption of visible light. Similar results were also obtained when CdSe QDs were used to sensitize TiO_2 nanotube arrays.²³ The maximum photocurrent is seen with 3.0 nm CdSe QDs. The optimal CdSe QDs have an absorption peak at 543 nm, which

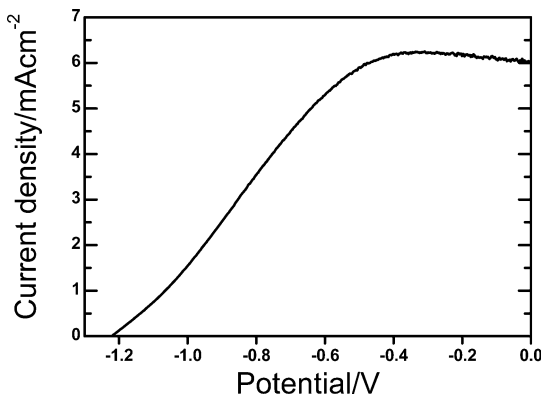


Figure 7. Current density–voltage characteristics measured from CdTe QDs (Q2)-sensitized TiO₂ nanotube photoelectrode with heat treatment.

is very close to that of CdTe QDs (536 nm) in our study. It is worth noting that for different kinds of QDs (CdTe and CdSe), the maximum photocurrents were all obtained when the QDs have an absorption peak around 540 nm.

Annealing the QDs-Modified TiO₂ Photoelectrode. The presence of the linker molecules between the CdTe QDs and TiO₂ nanotube can affect both the electronic structure at the interface and the electron transfer between CdTe QDs and TiO₂. To increase the photon-electric conversion efficiency further, the CdTe QD-sensitized samples were annealed at 300 °C in argon for 30 min. We note that the short-circuit current of the sample was increased significantly after the annealing, with the photocurrent onset occurring at −1.21 V and a large short-circle photocurrent of about 6 mA/cm² (Figure 7). Unlike in situ grown semiconductor QDs in the TiO₂ nanotube,^{11,27} the photocurrent increase after annealing may not be due to the improvement of the crystallinity of QDs or TiO₂ films, because in this case the TiO₂ nanotube film and CdTe QDs were both well crystallized before sensitization. And no obvious aggregation of nanoparticles was observed from the TEM images after this annealing process. Therefore, this significant improvement in the PEC cell performance may be largely attributed to the change in the interface between the CdTe QDs and TiO₂ nanotubes. After heat treatment, the organic linker molecules between CdTe QDs and TiO₂ nanotubes were vaporized (Scheme 1), leading to a narrower and better CdTe/TiO₂ interface that facilitates the photon-induced electrons being transferred more effectively to TiO₂ and decreases the loss in the electron transport process. It is noted that while the interfacial conduction band offset between TiO₂ and CdTe is much larger than that between TiO₂ and CdS, which is expected to reduce the cell conversion efficiency,³⁰ the photocurrent achieved here in this study is of the same order of magnitude as that from the CdS QDs/TiO₂ nanotube system.¹¹ It is expected that by further modifying the surface state of the TiO₂–CdTe interface and optimizing other factors, higher photoconversion efficiency could be obtained.

Conclusions

In summary, presynthesized inorganic CdTe QDs have been incorporated into TiO₂ nanotubes film and are shown to have significantly extended the photon response of the TiO₂ nanotube film electrodes into the visible region. The photoelectrochemical performance of the QDs-sensitized TiO₂ photoelectrode is affected significantly by the size of the CdTe QDs. Maximum

power conversion efficiency was obtained by CdTe QDs with an absorption peak at 536 nm. The photocurrent measured under AM 1.5G illumination is increased from 0.17 mA/cm² for the plain TiO₂ nanotube film to 6 mA/cm² for the CdTe QDs-sensitized film, presenting a 35 times improvement. This result confirms that CdTe QDs can be used as effective sensitizers and the photoconversion response can be readily tuned by controlling the CdTe size, and demonstrates the potential application of the TiO₂ nanotube/CdTe QD system in solar cells.

Acknowledgement .

This work was supported by the Ministry of Science and Technology (Grant No. 2006CB932401) and the National Science Foundation of China (Grant Nos. 90606026 and 60871002).

References and Notes

- (1) Fujishima, A.; Honda, K. *Nature (London)* **1972**, *238*, 37.
- (2) Mor, G. K.; Shankar, K.; Paulose, M.; Varghese, O. K.; Grimes, C. A. *Nano Lett.* **2005**, *5*, 191.
- (3) Park, J. H.; Kim, S.; Bard, A. J. *Nano Lett.* **2006**, *6*, 24.
- (4) Paulose, M.; Varghese, O. K.; Mor, G. K.; Grimes, C. A.; Ong, K. G. *Nanotechnology* **2006**, *17*, 398.
- (5) Mor, G. K.; Shankar, K.; Paulose, M.; Varghese, O. K.; Grimes, C. A. *Nano Lett.* **2006**, *6*, 215.
- (6) Paulose, M.; Shankar, K.; Varghese, O. K.; Mor, G. K.; Hardin, B.; Grimes, C. A. *Nanotechnology* **2006**, *17*, 1446.
- (7) Zhu, K.; Neale, N. R.; Miedaner, A.; Frank, A. J. *Nano Lett.* **2007**, *7*, 69.
- (8) Nozik, A. J. *Phys. E* **2002**, *14*, 115.
- (9) Vogel, R.; Hoyer, P.; Weller, H. *J. Phys. Chem.* **1994**, *98*, 3183.
- (10) Lin, S. C.; Lee, Y. L.; Chang, C. H.; Shen, Y. J.; Yang, Y. M. *Appl. Phys. Lett.* **2007**, *90*, 143517.
- (11) Sun, W. T.; Yu, Y.; Pan, H. Y.; Gao, X. F.; Chen, Q.; Peng, L. M. *J. Am. Chem. Soc.* **2008**, *130*, 1124.
- (12) Plass, R.; Pelet, S.; Krueger, J.; Gratzel, M. *J. Phys. Chem. B* **2002**, *106*, 7578.
- (13) Peter, L. M.; Wijayantha, K. G. U.; Riley, D. J.; Waggett, J. P. J. *Phys. Chem. B* **2003**, *107*, 8378.
- (14) Shen, Q.; Sato, T.; Hashimoto, M.; Chen, C.; Toyoda, T. *Thin Solid Films* **2006**, *499*, 299.
- (15) Robel, I.; Subramanian, V.; Kuno, M.; Kamat, P. V. *J. Am. Chem. Soc.* **2006**, *128*, 2385.
- (16) Zaban, A.; Micic, O. I.; Gregg, B. A.; Nozik, A. J. *Langmuir* **1998**, *14*, 3153.
- (17) Gao, M.; Kirstein, S.; Möhwald, H.; Rogach, A. L.; Kornowski, A.; Eychmüller, A.; Weller, H. *J. Phys. Chem. B* **1998**, *102*, 8360.
- (18) Gaponik, N.; Talapin, D. V.; Rogach, A. L.; Hoppe, K.; Shevchenko, E. V.; Kornowski, A.; Eychmüller, A.; Weller, H. *J. Phys. Chem. B* **2002**, *106*, 7177.
- (19) Macak, J. M.; Tsucak, H.; Schmuki, P. *Angew. Chem., Int. Ed.* **2005**, *44*, 2100.
- (20) Macak, J. M.; Tsuchiya, H.; Taveira, L.; Aldabergerova, S.; Schmuki, P. *Angew. Chem., Int. Ed.* **2005**, *44*, 7463.
- (21) Kamat, P. V.; Barazzouk, S.; Hotchandani, S. *Angew. Chem., Int. Ed.* **2002**, *41*, 2764.
- (22) Leschkies, K. S.; Divakar, R.; Basu, J.; Enache-Pommer, E.; Boercker, J. E.; Carter, C. B.; Kortshagen, U. R.; Norris, D. J.; Aydin, E. S. *Nano Lett.* **2007**, *7*, 1793–1798.
- (23) Kongkanand, A.; Tvrdy, K.; Takechi, K.; Kuno, M.; Kamat, P. V. *J. Am. Chem. Soc.* **2008**, *130*, 4007.
- (24) Dibbell, R. S.; Soja, G. R.; Hoth, R. M.; Watson, D. F. *Langmuir* **2007**, *23*, 3432–3439.
- (25) Balaur, E.; Macak, J. M.; Taveira, L.; Schmuki, P. *Electronchem. Commun.* **2005**, *7*, 1066.
- (26) Banerjee, S.; Mohapatra, S. K.; Das, P. P.; Misra, M. *Chem. Mater.* **2008**, *20*, 6784.
- (27) Seabold, J. A.; Shankar, K.; Wilke, R. H. T.; Paulose, M.; Varghese, O. K.; Grimes, C. A.; Choi, K. *Chem. Mater.* **2008**, *20*, 5266.
- (28) Robel, I.; Kuno, M.; Kamat, P. V. *J. Am. Chem. Soc.* **2007**, *129*, 4136.
- (29) Norris, D. J.; Bawendi, M. G. *Phys. Rev. B* **1996**, *53*, 16338.
- (30) Tiefenbacher, S.; Pettenkofer, C.; Jaegermann, W. *J. Appl. Phys.* **2002**, *91*, 1984.